

Effects of Lattice Types on the Frequency Band Widths in Photonic Crystals

Ahmed M. Kadhim
Ministry of Education/ Thi-Qar Government
Thi-Qar/ Iraq
ahmed_majphy@sci.utq.edu.iq

Hassan A. Yasser
College of Science / University of Thi-Qar
Thi-Qar/ Iraq
hahmha@yahoo.com

Abstract— The plane wave expansion method was implemented in modeling and simulating the band structures of two dimensional photonic crystals (PhCs) with square, triangular and honeycomb lattices with circular air holes in dielectric or circular GaAs rods in air. The eigen value equation of TE and TM modes will presented. The Fourier transform of dielectric constant will analyzed and the effects of lattice type will discussed. The eigenvalue equations of TE and TM modes will solved using Matlab environment. Our results show that the first type of PhCs is more flexible than the second type in controlling the band widths and the achieved frequency positions, and the triangular lattice showed the greatest flexibility. On the other hand, this work showed the significant effect of the dielectric constant and the lattice constant on the achieved bandwidth.

Keywords--Photonic crystal, lattice constant, dielectric constant.

I. INTRODUCTION

The study of periodic dielectric structure has received a lot of attention in recent years because of its ability to prevent electromagnetic waves from propagating in a specific frequency range [1]. This is owing to periodicity-induced reductions in degeneracies of free-photon states at the Bragg planes, which results in forbidden frequency gaps known as photonic band gaps (PBG) [2]. Despite the huge disparity in wavelengths, it is highly attractive to characterize the propagation of electromagnetic waves in these artificial materials in the same way as electron waves in actual crystals are [3]. The dispersion relation gives photonic band structures and some concepts, such as impurity states and effective masses, which are very usual for electrons, can be extended to photons. The existence of such PBGs when they overlap with the electronic gaps is particularly promising with regards to the control the spontaneous emission of light, which is essential for the realization of threshold less and low-noise semiconductor lasers. The study of structures that

possess wide PBGs in the frequency range of interest for the applications has motivated a lot of research [4].

To prevent wave propagation in any direction, the gaps opened at various points in the Brillouin zone must overlap as much as possible, resulting in large absolute band gaps. Thus, it is desirable that the different gaps are large and centered on neighboring frequencies. Such a condition can be achieved for the Brillouin zone by deviating slightly from the spherical shape [5]. The PhCs can play this role because they called PBGs. PBGs are frequency regions where light is forbidden to propagate. Thus, they allow for controlling over the photons similar to the one over charge carriers in electronics [6]. To be practical, PBGs should be active for both transverse electric (TE) and transverse magnetic (TM) polarizations at all angles of light incidence [7]. Two dimensional (2D) PhCs can exhibit a variety of such PBGs. However, idealized 2D PhCs are not realistic and are used only for computational modeling. There are two main types of PhC structures: the first type is high dielectric index pillars in air that tends to open TM PBGs, and the second type is air holes in high dielectric background that tends to open TE PBGs [8,9].

In this paper, the eigen value equation of TE and TM modes will presented. The Fourier transform of ϵ dielectric constant will analyzed and the effects of lattice type and rod shapes will discussed. We will focus on two types of PhCs, the first is circular air holes in dielectric and the second is a GaAs circular rods that were arranged in air.

II. THEORETICAL MANAGEMENT

Essentially, there are types of 2D lattice structures: the orthogonal lattice and the oblique lattice. The orthogonal lattice is shown in Fig. 1a, which is called '2D square lattice'. In the oblique systems, there are the triangular lattice (also called as a hexagonal lattice) shown in Fig. 1b and the honeycomb lattice is shown in Fig. 1c [10].

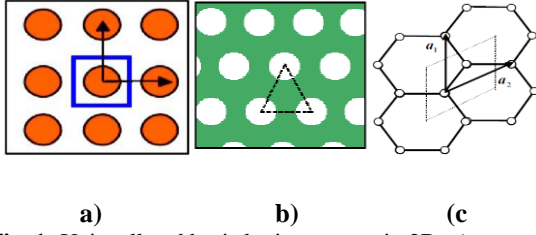


Fig. 1: Unit cell and basis lattice vectors in 2D: a) square b) triangular c) honeycomb lattices [1].

The photonic band structures can be obtained by solving Maxwell's equations using the plane wave expansion method. For the sake of convenience, we provide a brief account of this method. Consider a periodic array of circular dielectrics with longitudinal axes parallel to the z -axis. In terms of dielectric materials, Maxwell's equations are represented in terms of the magnetic field H [9]

$$\nabla \times \frac{1}{\varepsilon(\mathbf{r})} \nabla \times \mathbf{H}(\mathbf{r}) = \frac{w^2}{c^2} \mathbf{H}(\mathbf{r}) \quad (1)$$

where ε is the position-dependent dielectric constant, r is the coordinates in the plane perpendicular to the rods, and c is the EM wave phase speed in a vacuum. For infinite periodic structures, Bloch theorem is often used [10]. The Bloch theorem shows that a plane wave in an infinite periodic structure will be modulated by periodicity. So, the magnetic field can be expressed as [11]

$$\mathbf{H}(\mathbf{r}) = h(\mathbf{r}) e^{i\mathbf{k} \cdot \mathbf{r}} \hat{e}_k = h(\mathbf{r} + \mathbf{L}) e^{i\mathbf{k} \cdot \mathbf{r}} \hat{e}_k \quad (2)$$

where \mathbf{L} is an arbitrary lattice vector, \hat{e}_k is a unit vector in the direction of \mathbf{H} and perpendicular to the wave vector \mathbf{k} . The dielectric function $\varepsilon(\mathbf{r})$ is periodic in r -space $\varepsilon(\mathbf{r}) = \varepsilon(\mathbf{r} + \mathbf{L})$, where $\mathbf{L} = l_1 \mathbf{a}_1 + l_2 \mathbf{a}_2 + l_3 \mathbf{a}_3$, $l_i, i=1,2,3$ are integers, and $\mathbf{a}_i, i=1,2,3$ are the basis vectors to describe the periodic lattice. The Fourier transform for periodic functions may be written as [3]

$$\frac{1}{\varepsilon(\mathbf{r})} = \sum_{\mathbf{G}} \kappa(\mathbf{G}) e^{i\mathbf{G} \cdot \mathbf{r}} \leftrightarrow \kappa(\mathbf{G}) = \frac{1}{A} \int_{\Omega} \frac{1}{\varepsilon(\mathbf{r})} e^{-i\mathbf{G} \cdot \mathbf{r}} d\Omega \quad (3)$$

where $A = \mathbf{a}_1 \cdot \mathbf{a}_2 \times \mathbf{a}_3$ corresponds to the volume of the PhC unit cell. Since $h(\mathbf{r})$ has the same periodic property as $\varepsilon(\mathbf{r})$, the magnetic field can be extended as [4]

$$\mathbf{H}(\mathbf{r}) = \sum_{G_i, \lambda} h_{G_i, \lambda} e^{i(\mathbf{k} + \mathbf{G}_i) \cdot \mathbf{r}} \hat{e}_\lambda \quad (4)$$

Here, G_i is an arbitrary spatial frequency which we call it as reciprocal lattice vector and $\mathbf{G}_i = h_1 \mathbf{b}_1 + h_2 \mathbf{b}_2 + h_3 \mathbf{b}_3$, where $h_i, i=1,2,3$ are integers, $\mathbf{b}_i, i=1,2,3$ represent basis vectors in the reciprocal space, λ takes the values 1 and 2, \hat{e}_λ represents the two orthogonal unit

vectors, $\hat{e}_1 \cdot \hat{e}_2 = 0$, which are perpendicular to $\mathbf{k} + \mathbf{G}_i$, i.e. $(\mathbf{k} + \mathbf{G}_i) \cdot \hat{e}_\lambda = 0$.

Using Eqs.(4) into (1), yields [12]

$$\sum_{\mathbf{G}'} |\mathbf{k} + \mathbf{G}'| |\mathbf{k} + \mathbf{G}| \kappa(\mathbf{G} - \mathbf{G}') \begin{bmatrix} \hat{e}_2 \cdot \hat{e}'_2 & -\hat{e}_2 \cdot \hat{e}'_1 \\ -\hat{e}_1 \cdot \hat{e}'_2 & \hat{e}_1 \cdot \hat{e}'_1 \end{bmatrix} \begin{bmatrix} h'_1 \\ h'_2 \end{bmatrix} h = \frac{w^2}{c^2} \begin{bmatrix} h_1 \\ h_2 \end{bmatrix} \quad (5)$$

Since $\hat{e}_2 \cdot \hat{e}'_1 = \hat{e}_1 \cdot \hat{e}'_2 = 0$ are zero, and two polarizations h_1 and h_2 become decoupled. Where h_1 is in the xy -plane and h_2 is along z -direction, h_1 is TM mode, and h_2 is TE mode. For 2D lattices, the material is homogeneous in z direction while periodic along x and y directions. The mirror symmetry along the z axis allows to classify the modes by separating them into two distinct polarization, the TE mode and the TM mode. Therefore Eq.(5) decoupled into two equations which makes two unit vector sets unnecessary. The TM polarized mode and TE-polarized mode will be [8]

$$TM \quad \sum_{\mathbf{G}'} |\mathbf{k} + \mathbf{G}'| |\mathbf{k} + \mathbf{G}| \kappa(\mathbf{G} - \mathbf{G}') h_1(\mathbf{G}') = \frac{w^2}{c^2} h_1(\mathbf{G}) \quad (6a)$$

$$TE \quad \sum_{\mathbf{G}'} (\mathbf{k} + \mathbf{G}') \cdot (\mathbf{k} + \mathbf{G}) \kappa(\mathbf{G} - \mathbf{G}') h_2(\mathbf{G}') = \frac{w^2}{c^2} h_2(\mathbf{G}) \quad (6b)$$

The absolute parts of these fields are used to calculate mode fields. $\kappa(\mathbf{G})$ is the inverse of the Fourier transform matrix of $\varepsilon(\mathbf{r})$. In this standard eigenvalue problem, the difficulty in the analysis of the eigenvalue problem lies on Fourier transformation of the dielectric function. Performing a numerical fast Fourier transform is subjected to convergence problem and symmetry conditions become complex for some problems [6]. The Fourier component, in the lattice space of dielectric constant $\varepsilon(\mathbf{r})$ is defined as [8]

$$\varepsilon(\mathbf{r}) = \begin{cases} \varepsilon_b & \text{if } r > R \\ \varepsilon_a & \text{if } r \leq R \end{cases} = \varepsilon_b + \begin{cases} 0 & \text{if } r > R \\ \varepsilon_a - \varepsilon_b & \text{if } r \leq R \end{cases} \quad (7)$$

where R is the air cylinder radius. Substituting Eq.(7) into (3) and simplification the result yields [13]

$$\kappa(\mathbf{G}) = \begin{cases} \frac{f}{\varepsilon_a} + \frac{f-1}{\varepsilon_b} & \mathbf{G} = 0 \\ 2f \left(\frac{1}{\varepsilon_a} - \frac{1}{\varepsilon_b} \right) \frac{J_1(GR)}{GR} & \mathbf{G} \neq 0 \end{cases} \quad (8)$$

where f is the filling factor defined as the fraction of area occupied by the localized medium in one unit cell, and $J_1(GR)$ is the first-class Bessel function and $(\varepsilon_a$ and $\varepsilon_b)$ refer to the dielectric constants of the localized medium and the background respectively.

For honeycomb lattice, $\kappa(\mathbf{G})$ is given by [7]

$$\kappa(G) = \begin{cases} \frac{f}{\varepsilon_a} + \frac{f-1}{\varepsilon_b} & \overset{r}{G} = 0 \\ 2f \left(\frac{1}{\varepsilon_a} - \frac{1}{\varepsilon_b} \right) \cos \chi \frac{J_1(GR)}{GR} & \overset{r}{G} \neq 0 \end{cases} \quad (9)$$

where the parameter χ is defined as

$$\chi = \frac{a}{2}(G_x - G'_x) + \frac{a}{2\sqrt{3}}(G_y - G'_y) \quad (10)$$

where G_x, G'_x, G_y, G'_y are vectors that constructed from the reciprocal lattice vectors and a is the lattice constant. The difference between Eq.(8) and (9) is that the factor $\cos \chi$ appears in the case of honeycomb PhC [10]. The structure factors for various shapes are tabulated in table(1).

TABLE. 1: Examples of Structure Factors for Different Shapes of Rods [10].

Shape	Structure Factor
Circular	$2f \frac{J_1(GR)}{GR}$ where R is the radius of cylinder
Square rod	$f \operatorname{sinc}(G_x a / 2) \operatorname{sinc}(G_y a / 2)$ where $\operatorname{sinc}(x) = \sin x / x$ and a is the side-length of a square
Honeycomb rod	$\frac{2f}{3aG_x} \left\{ \begin{aligned} &\sin \frac{a}{4}(3G_x + \sqrt{3}G_y) \operatorname{sinc} \frac{a}{4}(G_x - \sqrt{3}G_y) \\ &+ \sin \frac{a}{4}(3G_x - \sqrt{3}G_y) \operatorname{sinc} \frac{a}{4}(G_x + \sqrt{3}G_y) \end{aligned} \right\}$ where a is the side-length of a hexagonal

III. RESULTS and DISCUSSION

The calculations were performed using the Matlab environment using the values: $\varepsilon_a = 1, \varepsilon_b = 13$ in the first type and $\varepsilon_a = 8, \varepsilon_b = 1$ in the second type, unless otherwise indicated. Emphasis is placed on computing the band width in the two cases. Noting that the method adopted for the solution is not ideal like other methods, but it is the best method to solve the wave equations in the PhCs. Figs. 2 and 3 explain the normalized band width as function of ε_b of the first type of TE and TM modes using the lattices: square, triangular and honeycomb, respectively. For all cases, the larger ε_b value may present larger band width for a significant bands. In general, ε_b may be maximized one band except the case (square lattice) in the TE modes. For a square lattice, Fig. 2 shows that the first and second bands will occur, where the width of the band increases with the increase in the permittivity ε_b , while noting that the width of the second band is greater. For triangular lattice, the first band width increases with increase ε_b , and a little secondary width is achieved for other bands. In the case of honeycomb lattice, the fourth band appears to give the greatest width. Fig. 3 represents the TM modes of the first

type of PhCs, in the case of a square lattice, one can see that only the first band will occur, where the width of the band increases with the increase of ε_b . In the case of triangular lattice, the seventh band appears to give the greatest width at $\varepsilon_b = 13$, and the sixth band can appear less frequently. In the case of honeycomb lattice, the first band appears to give the greatest width increases with increase ε_b , and the fifth band appears with a smaller width and is the greatest possible at $\varepsilon_b = 8$. Note that, the dielectric value ε_b may be used to control the band width but the allowed values of permittivity are limited for dielectric, where we find that the triangular lattice at $\varepsilon_b = 13$ has the largest width.

Figs. 4 and 5 explain the normalized band width as a function of ε_a of the second type of TE and TM modes using the lattices: square, triangular and honeycomb, respectively. For all cases, the larger ε_a value may present larger band width for a significant bands. In the case of the square lattice, Fig. 4 indicates that the largest band width appears at the sixth band at $\varepsilon_a = 6$, and there is little width achieved at the fourth band within a small range of the permittivity which is greatest possible at $\varepsilon_a = 8$. For triangular lattice, the first band width increases with increase ε_a , and a little secondary width is achieved for other bands. In the case of honeycomb lattice, it does not show any band, and therefore this case will not pass the electric field at all. Here the triangular lattice achieves better width than the other lattices. In Fig. 5, the third, sixth, and first bands appear almost identically in the case of the square lattice and triangular lattice, and not appear in the case of the honeycomb lattice. One can see that the bands appear to give the greatest width increases with increase ε_a . Here again the second type PhC never passes the magnetic field. Note that, the dielectric value ε_a may be used to control the band width but the allowed values of permittivity are limited for dielectric. We find that the triangular lattice at $\varepsilon_a = 8$, has the largest width.

Fig. 6 explains the photonic band structures for one IBZ of the TE modes of the first type for the lattices: square, triangular and honeycomb. The complet bands present in the different lattices at different locations. Also, the band width affects by lattice type. In general, electromagnetic waves in periodic structures only exist as discrete modes, These are called Bloch modes. Fields can only exist as integer combinations of the eign-modes of the lattice. Electric field the of the lowest order mode refere to reside in higher index regions. Modes must be orthogonal. However, the present band gap structures compute at the radius $R = 0.38a$ of the air holes in the first type. These photonic band structures will be changed strongly by changing the lattice parameters.

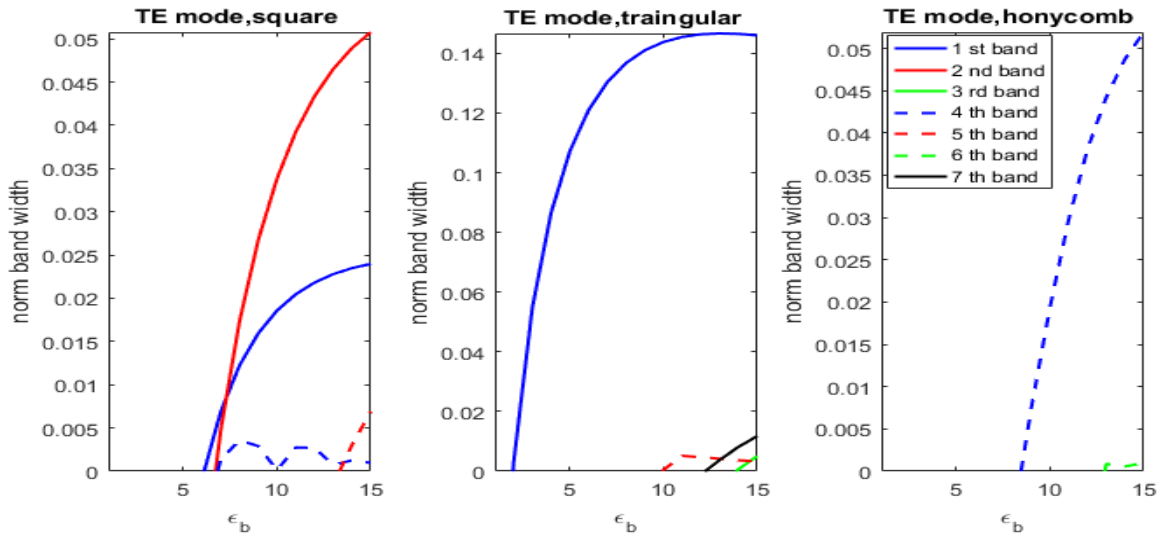


Fig. 2: The normalized band width of TE modes in first type lattice as function of ϵ_b for $R = 0.38a$.

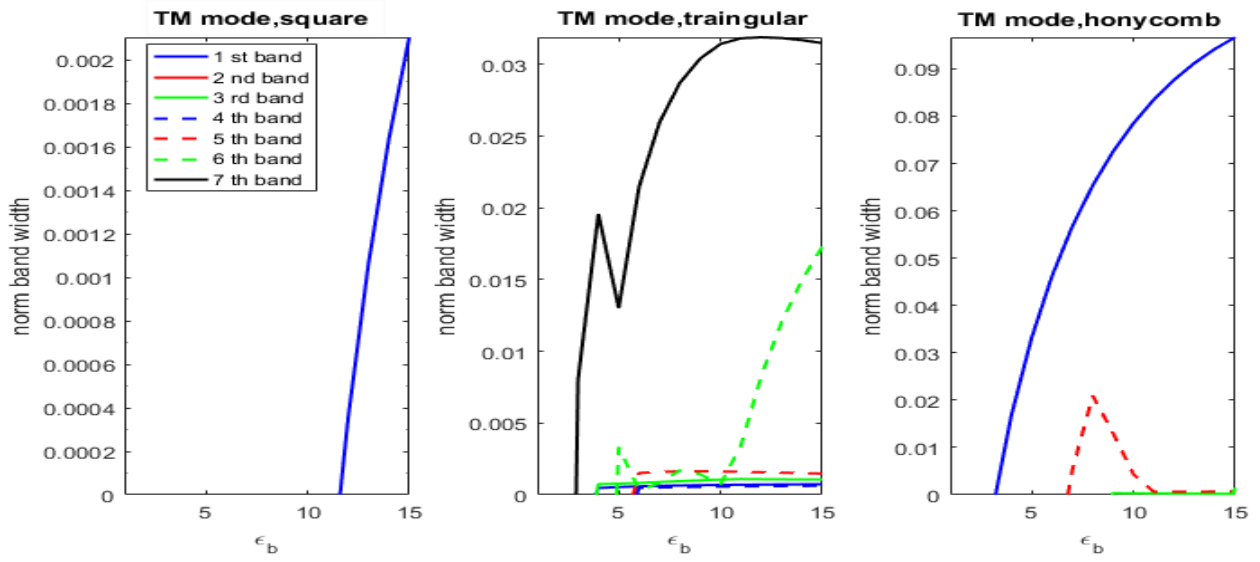


Fig. 3: The normalized band width of TM modes in first type lattice as function of ϵ_b for $R = 0.38a$.

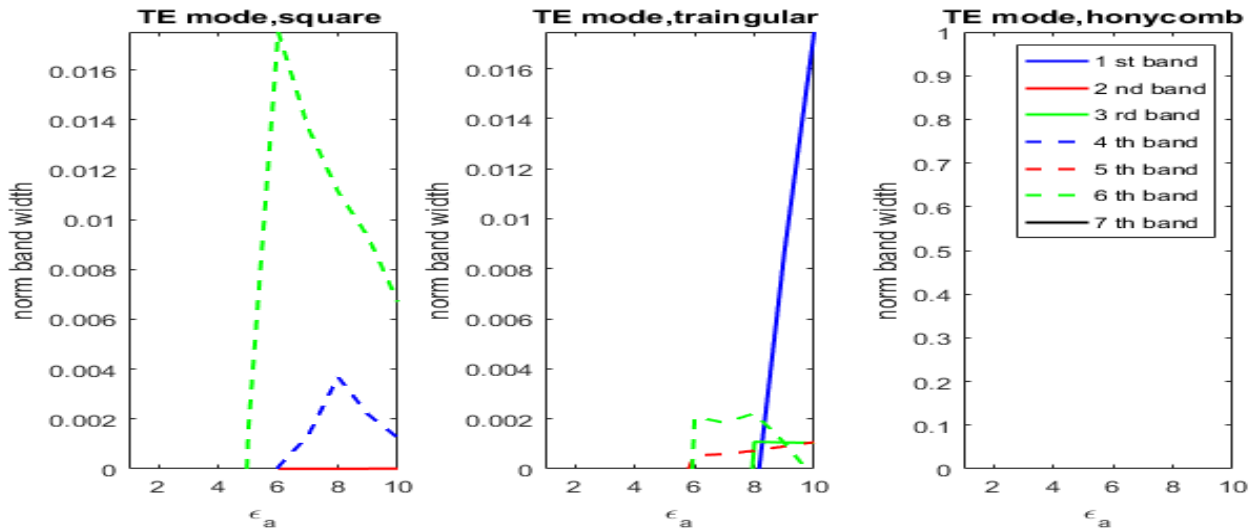


Fig. 4: The normalized band width of TE modes in second type lattice as function of ϵ_a for $R = 0.38a$.

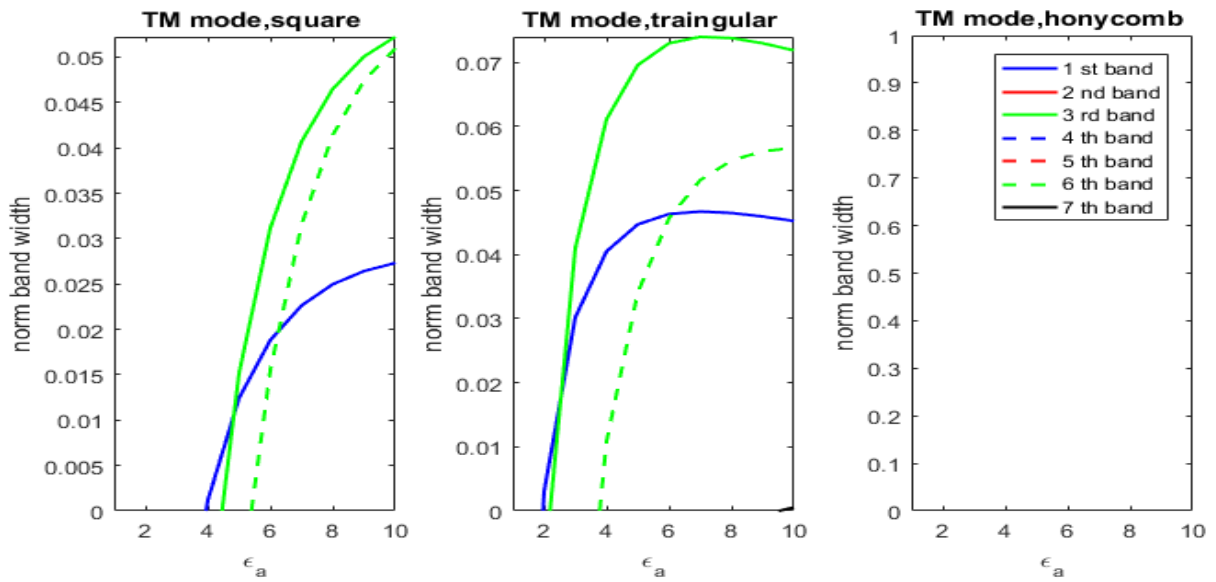


Fig. 5: The normalized band width of TM modes in second type lattice as function of ϵ_a for $R = 0.38a$.

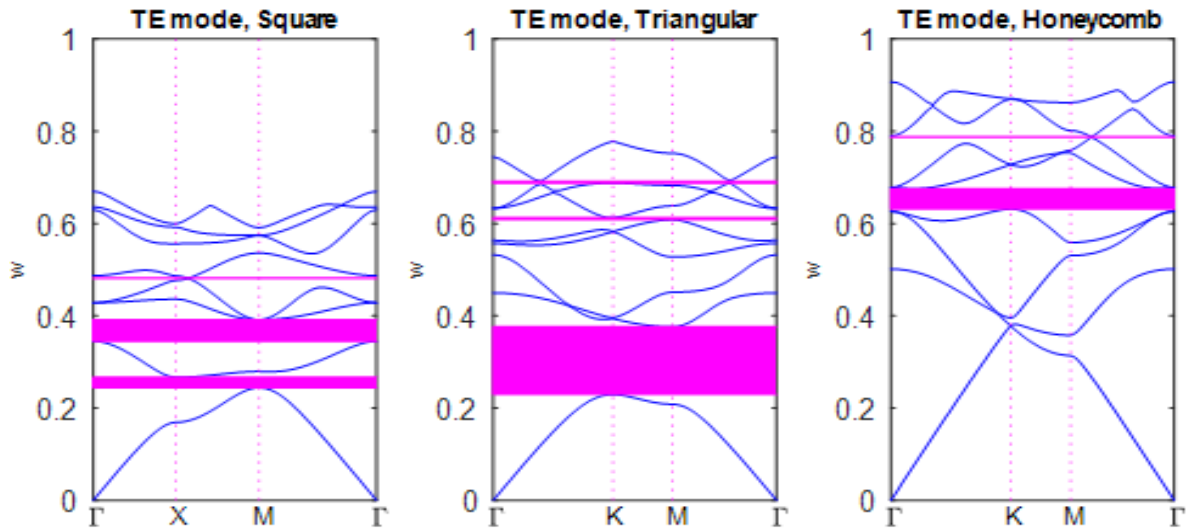


Fig. 6: Band structures of TE modes in 2D PhC lattices with radius $R=0.38a$ for the first type.

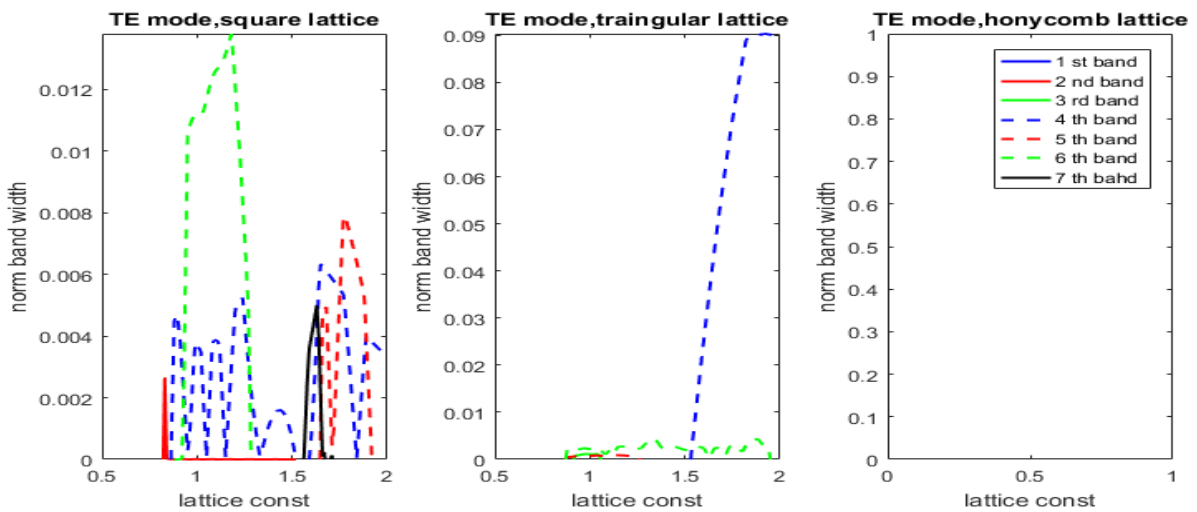


Fig. 7: The norm band width as a function of lattice constant for $R = 0.38a$ of TE modes in second type lattice.

Fig. 7 illustrates the normalized band width as a function of lattice constant for the TE modes using different lattices in the first type PhC. The lattice constant can control the band width for any lattice. In the case of a square lattice, a greater width occurs at the sixth band in the lattice constant 1.2, and an oscillating secondary width at the fourth band. In the case of triangular lattice, a greater width occurs at the fourth band that appears at lattice constant 1.9, and a little secondary width is achieved for other bands. In the case of honeycomb lattice, it does not show any band, and therefore this case will not pass the electric field at all. That is; the triangular lattice has the largest width.

IV. CONCLUSIONS

As a conclusion, the achieved complete bands are affected by the PhC type, the lattice type, and the lattice constant. The dielectric constant and lattice constant must be regulated in order to maximize the achievable bandwidth. Maximum bandwidths are reached in the first type due to a larger dielectric constant than in the other type. In general, the TM band gaps are favored in a lattice of isolated high- ϵ regions and TE band gaps are favored in a connected lattice.

ACKNOWLEDGEMENT

I would like to thank who got tired because of my lack of knowledge and he was as my a father in his efforts. (**Prof. Dr. Hassan Abid Yasser**) my supervisor and for guiding my thesis, despite the difficulties we have faced.

REFERENCES

- [1] J. Joannopoulos, S. Johnson, J. Winn and R. Meade, "Photonic crystals Molding the flow of light", Copxright, Second Edition, 2008.
- [2] A. Sukhoivanov and V. Guryev, "Physics and Practical Modeling", Springer, 2009.
- [3] D. Szymanski, S. Patela, "Modelling of Photonic Crystals", 2005 International Students and Young Scientists Workshop, pp.79-82, 2014.
- [4] P. Sivarajah, A. Maznev, B. Ofori-Okai and K. Nelson, "What is the Brillouin zone of an anisotropic photonic crystal", Physical Review, Vol. 93, pp.054204, 2016.
- [5] Ch. Liu, X. Kong and Sh. Liu, "Band gap extension in honeycomb lattice two-dimensional plasma photonic crystals in the presence of dissipation", Optik, Vol.124, pp.4989-4993, 2013.
- [6] L. Kassa, "Photonic Band Gap Analysis of Silicon Photonic-Crystal Slab Structures with Non-Circular Air Holes", Acta Physica Polonica, Vol. 138, No. 3, 2020.
- [7] S. Hassan, Y. Jiang, K. Alnasser, N. Hurley, H. Zhang, U. Philipose and Y. Lin, "Generation of over 1000 Direction Spots from 2D Graded Photonic Super-Crystals", Photonics, pp. 1-8, 2020.
- [8] K. Sakoda, "Optical Properties of Photonic Crystals", springer, Second Edition, 2005.
- [9] F. Segovia and H. Vinck, "Dependence of photonic defect modes on hydrostatic pressure in a 2D hexagonal lattice", Physica E: Low-dimensional Systems and Nanostructures, Vol.104, pp.49-57, 2018.
- [10] S. Dissanayake and K. Wijewardena, "Simulation of Two Dimensional Photonic Band Gaps", International Letters of Chemistry, Physics and Astronomy, No.5, pp.58-88, 2014.
- [11] F. Segovia, H. Vinck and E. Navarro, "Photonic band structure in a two-dimensional hexagonal lattice of equilateral triangles" Physics Letters, Vol. 383, pp. 3207–3213, 2019.
- [12] K. Jayawardana and K. Gamalath, "Study on the Photonic Band Gaps of the Face Centered Cubic Crystals" International Letters of Chemistry, Vol. 70, pp.63-75, 2016.
- [13] Y. Zong and J. Xia, "Photonic band structure of two-dimensional metal/dielectric photonic crystals", Phys, Vol. 48, 2015.